

# INFORMATION TECHNOLOGIES ИНФОРМАЦИОННЫЕ ТЕХНОЛОГИИ



UDC 519.6

Original Theoretical Research

<https://doi.org/10.23947/2587-8999-2026-10-1-58-71>



## Oil Spill Detection Based on Enhanced LBP Neural Algorithms for Noisy Satellite Images

Alexander I. Sukhinov , Denis A. Solomakha , Valentina V. Sidoryakina

Don State Technical University, Rostov-on-Don, Russian Federation

✉ [cvv9@mail.ru](mailto:cvv9@mail.ru)

### Abstract

**Introduction.** Detecting oil spills in satellite imagery presents a significant challenge due to the low visual contrast between oil slicks and the sea background, particularly under varying illumination conditions and sensor noise. Traditional approaches typically convert RGB images to grayscale prior to texture analysis, discarding wavelength data critical for distinguishing oil types and thicknesses. This paper proposes a novel approach to processing each Local Binary Pattern (LBP) channel using a Pyramid Scene Parsing Network (PSPNet) architecture, which processes each RGB channel independently, preserving the spectral-textural characteristics necessary for accurate oil spill identification.

**Materials and Methods.** The modified approach retains three parallel LBP streams that capture channel-specific texture patterns, which are concatenated with the original RGB input to form a six-channel tensor for deep learning processing. Training incorporates comprehensive noise augmentation strategies simulating real-world remote sensing conditions.

**Results.** Experimental validation demonstrates that the proposed approach achieves a mean Intersection over Union (mIoU) of 86.05% on the test dataset, representing a 3.25% improvement over traditional grayscale LBP implementations. Critically, the presented model exhibits exceptional noise robustness compared to models based on conventional approaches.

**Discussion.** The per-channel processing strategy effectively distinguishes thin oil films from spill-like phenomena (sun glint on the water surface, wind-induced disturbances).

**Conclusion.** The results obtained in this study contribute to the development of operational oil spill monitoring systems requiring reliable performance under diverse environmental conditions and imaging scenarios.

**Keywords:** PSPNet, LBP, oil spill detection, image segmentation

**Funding.** The study was supported by the Russian Science Foundation grant No. 22–11–00295–II, <https://rscf.ru/en/project/22-11-00295/>

**For Citation.** Sukhinov A.I., Solomakha D.A., Sidoryakina V.V. Oil Spill Detection Based on Enhanced LBP Neural Algorithms for Noisy Satellite Images. *Computational Mathematics and Information Technologies*. 2026;10(1):58–71. <https://doi.org/10.23947/2587-8999-2026-10-1-58-71>

Оригинальное теоретическое исследование

## Обнаружение разливов нефти на основе усовершенствованных LBP-нейроалгоритмов для зашумленных космических снимков

А.И. Сухинов , Д.А. Соломаха , В.В. Сидорякина

Донской государственный технический университет, г. Ростов-на-Дону, Российская Федерация

✉ [cvv9@mail.ru](mailto:cvv9@mail.ru)

### Аннотация

**Введение.** Обнаружение разливов нефти на спутниковых изображениях представляет собой значительную проблему из-за низкого визуального контраста между нефтяными пятнами и морским фоном, особенно при изменя-

ющихся условиях освещения и шумах датчиков. Традиционные подходы обычно преобразуют *RGB*-изображения в оттенки серого перед анализом текстуры, отбрасывая данные о длине волны, критически важные для различения типов и толщины нефти. В настоящей работе предложен новый подход к обработке каждого канала *Local Binary Pattern (LBP)* с архитектурой *Pyramid Scene Parsing Network (PSPNet)*, который обрабатывает каждый *RGB*-канал независимо, сохраняя спектрально-текстурные характеристики, необходимые для точной идентификации нефтяных разливов.

**Материалы и методы.** Модифицированный подход сохраняет три параллельных потока *LBP*, которые фиксируют текстурные паттерны, специфичные для каждого канала, и объединяются с исходным *RGB*-входом для формирования шестиканального тензора при обработке глубоким обучением. Обучение включает комплексные стратегии увеличения шума, имитирующие реальные условия дистанционного зондирования.

**Результаты исследования.** Экспериментальная проверка показывает, что данный подход достигает среднего значения пересечения по объединению (mIoU) 86,05 % на тестовом наборе данных, что представляет собой улучшение на 3,25 % по сравнению с традиционными реализациями *LBP* в оттенках серого. Критически важно, что представленная модель демонстрирует исключительную устойчивость к шуму по сравнению с моделями, основанными на традиционных подходах.

**Обсуждение.** Стратегия обработки по каналам эффективно отличает тонкие нефтяные пленки от явлений, похожих на разливы (блики солнца на поверхности воды, ветровое волнение).

**Заключение.** Полученные в работе результаты вносят вклад в разработку систем оперативного мониторинга нефтяных разливов, требующих надежной работы в различных природных условиях и сценариях съемки.

**Ключевые слова:** *PSPNet*, *LBP*, обнаружение разлива нефти, сегментация изображений

**Финансирование.** Исследование выполнено за счет гранта Российского научного фонда № 22-11-00295-П, <https://rscf.ru/project/22-11-00295/>

**Для цитирования.** Сухинов А.И., Соломаха Д.А., Сидорякина В.В. Обнаружение разливов нефти на основе усовершенствованных *LBP*-нейроалгоритмов для зашумленных космических снимков. *Computational Mathematics and Information Technologies*. 2026;10(1):58–71. <https://doi.org/10.23947/2587-8999-2026-10-1-58-71>

**Introduction.** Oil spills represent one of the most severe environmental problems associated with the extraction and transportation of hydrocarbons, causing devastating impacts on marine ecosystems, recreational systems, and coastal economies [1–4]. Even minor oil spills can lead to the formation of large slicks that are transported by currents to sandy beaches extending along a third of the world’s coastlines [4]. Toxic components of oil disrupt photosynthetic processes and adversely affect living organisms inhabiting marine waters [5–9].

To minimize damage, the timely detection and localization of spills are critically important. Traditional methods, such as sampling and contact surveys, have limitations related to the coverage of water areas, lack of operational speed, and high cost [4]. Remote sensing through satellite imagery, radar data, and aerial photography provides a viable alternative. However, the accuracy of such approaches depends on the complexity of the spill’s shape, size, and propagation direction, particularly for remote marine areas [10].

Building upon [11, 12], the authors fundamentally improve the *LBP* processing pipeline by modifying it from a grayscale-based implementation to a per-channel processing strategy with integrated noise robustness mechanisms. The original *LBP+PSPNet* model converted the *RGB* input to grayscale prior to *LBP* computation, resulting in the loss of valuable channel-specific textural information. In the enhanced approach, each color channel is processed independently, preserving wavelength-dependent texture that is critical for distinguishing oil slicks from similar background patterns. This architectural improvement directly addresses a key limitation in the previous implementation, where channel-specific texture information was lost during the grayscale conversion process, significantly enhancing the model’s ability to discriminate between various oil types and background elements under complex environmental conditions.

The per-channel *LBP* implementation provides three critical advantages over the traditional grayscale approach. First, the *LBP* for the blue channel captures oil-water boundary patterns that are invisible in grayscale representations, as oil absorbs blue wavelengths differently than water [10]. This is particularly valuable for detecting thin oil films, where spectral differences are most pronounced in the blue spectrum. Second, the *LBP* for the red channel reveals subtle textural variations associated with oil thickness variations, since thicker oil accumulates greater red light absorption, creating characteristic patterns that are averaged out during grayscale conversion [9]. Third, the green channel processing captures mid-spectrum interactions that provide complementary information to the other channels, improving overall discriminative capability in complex coastal scenarios.

The computational cost of the developed approach is minimal compared to the original method. This efficiency is maintained because the per-channel *LBP* is implemented as three parallel convolutional layers with fixed weights,

avoiding the need for additional trainable parameters [13, 14]. The model’s ability to exploit channel-specific texture patterns while maintaining noise robustness represents a significant advancement for operational oil spill monitoring systems. The method is practical for real-time applications where computational resources are limited, delivering superior performance in complex detection scenarios.

**Materials and Methods**

**Dataset Overview.** The dataset used in this study consists of RGB images specifically curated for oil spill detection and classification tasks. The final dataset comprises 8,376 training, 41 validation, and 75 test images, standardized to a uniform resolution of 512×512 pixels through systematic preprocessing.

The dataset includes four distinct oil classes, each characterized by specific visual properties corresponding to different oil thicknesses: black oil represented as (255, 255, 255), brown oil as (180, 180, 180), iridescent oil as dark yellow (123, 123, 123), light yellow as silver (123, 123, 123), and background represented as (0, 0, 0). This multi-class structure enables not only detection but also quantification of different oil thicknesses, providing critically important information for environmental response planning.

The annotation methodology follows semantic segmentation principles, with small gaps intentionally maintained between adjacent oil regions to ensure accurate boundary classification. Each image contains carefully selected oil regions constituting 20% to 90% of the total image area, providing meaningful training samples while avoiding ambiguous cases with minimal or excessive oil coverage.

The test set was specifically curated to include challenging scenarios with small oil slicks, sun glint interference, and images containing multiple oil types, providing a rigorous evaluation framework for model performance. This comprehensive dataset represents a unique resource for oil spill classification, as it systematically categorizes oil types based on visual characteristics rather than focusing exclusively on binary oil/background detection.

**Proposed Modified LBP Algorithm.** The traditional LBP approach typically converts RGB images to grayscale prior to texture analysis, resulting in the loss of color channel information. To overcome this limitation, the authors propose a modified LBP algorithm that processes each color channel independently while preserving the original color information. This approach retains the distinct textural characteristics present in each spectral band, which is particularly important for oil spill detection, where different oil types exhibit unique spectral signatures.

Let  $I_{RGB}(x, y) = [R(x, y), G(x, y), B(x, y)]$  denote the RGB image at pixel coordinates  $(x, y)$ . For each channel  $c \in \{R, G, B\}$  the modified LBP operator is defined as:

$$LBP_c(x, y) = \sum_{k=1}^8 s(p_k^c - p_c^c) \cdot 2^{k-1}, \tag{1}$$

where  $p_c^c$  is the value of the central pixel in channel  $c$ ;  $p_k^c$  is the  $k$ -th neighboring pixel in the same channel; and  $s$  is the thresholding function:

$$s = s(x) = \begin{cases} 1, & \text{ecnu } x > 0, \\ 0, & \text{ecnu } x \leq 0. \end{cases} \tag{2}$$

This operation is performed separately for each of the three color channels, resulting in three distinct LBP maps:  $LBP_R, LBP_G, LBP_B$ . Unlike the traditional approach, which aggregates color information through grayscale conversion, the authors’ method preserves complete color-texture information through independent processing of each channel.

The modified algorithm employs a fixed 3×3 neighborhood configuration, where the central pixel is compared with its eight immediate neighbors [15]. The binary pattern generated for each pixel is subsequently converted into a decimal value representing the local texture pattern. This process is repeated for all pixels in each channel, producing three texture maps that capture channel-specific textural information.

**Enhanced Texture Representation.** The proposed independent channel-wise LBP processing approach provides a substantially richer texture representation compared to traditional grayscale-based methods. By preserving separate texture analysis for each RGB channel, the algorithm captures color-dependent textural characteristics that are crucial for distinguishing oil spills from look-alike phenomena, such as sun glint or biological films.

The three-channel texture representation  $LBP_{RGB}(x, y) = [LBP_R(x, y), LBP_G(x, y), LBP_B(x, y)]$  retains unique texture signatures associated with different oil thicknesses and types. For instance, silver oil typically exhibits distinctive texture patterns in the blue channel, while iridescent oil displays characteristic patterns across all three channels. This color-specific textural information provides additional discriminative features that enhance the model’s ability to differentiate between oil types and background elements.

The enhanced texture representation can be integrated into deep learning architectures by concatenating the three LBP maps with the original RGB image, forming a six-channel input tensor. This enriched input enables the network to leverage both spectral and textural information simultaneously, significantly improving segmentation performance under challenging conditions where visual contrast between oil and water is minimal.

Experimental results demonstrate that this independent channel processing approach increases the IoU metric by 3.25% compared to traditional grayscale LBP, particularly improving the detection of silver and iridescent oil, which previously suffered from high false positive rates due to their similarity to sun glint and other background elements.

**Model Architecture.** The proposed model architecture integrates channel-independent LBP texture extraction with a ResNet101-based backbone and PSPNet for enhanced oil spill segmentation. The model processes a six-channel input tensor that concatenates the original RGB channels with three separate LBP channels computed independently for each color channel.

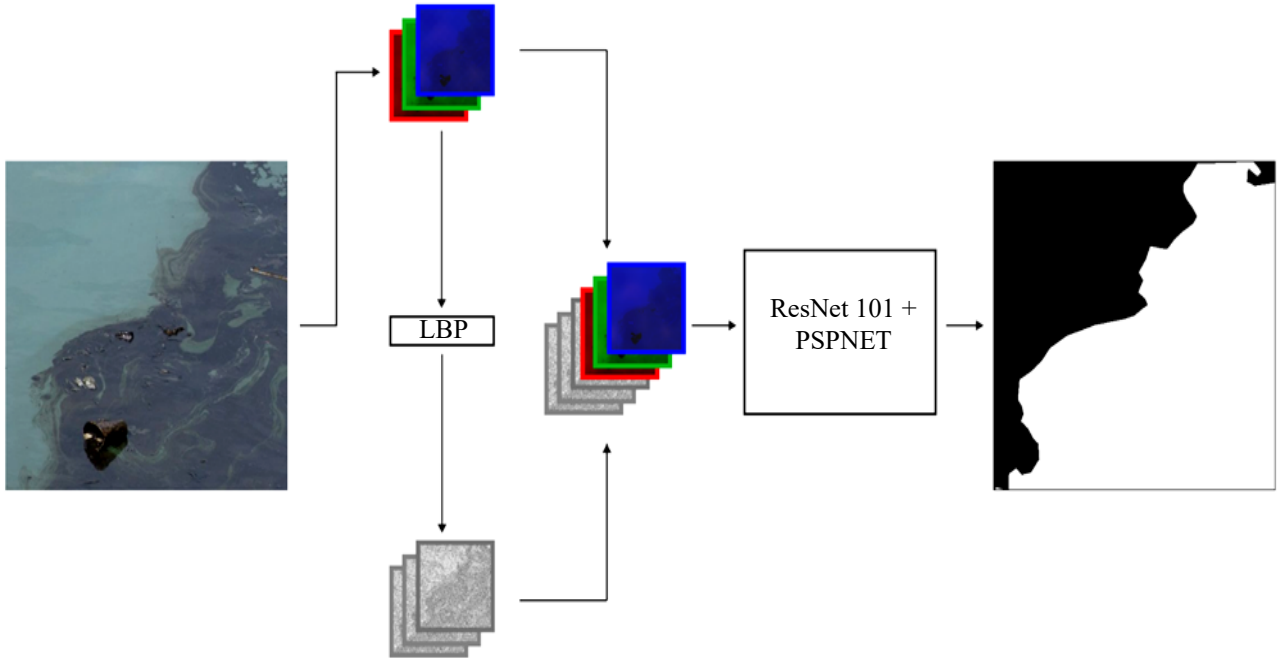


Fig. 1. LBP + PSPNet architecture

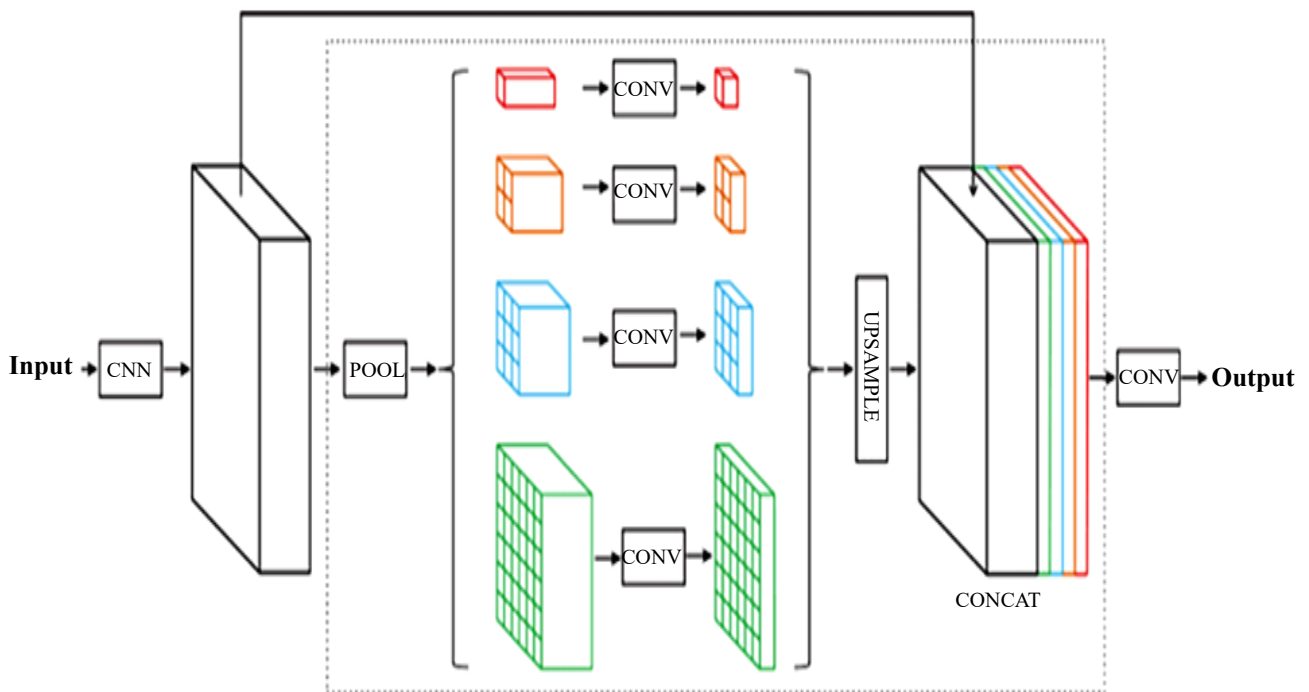


Fig. 2. PSPNet architecture

The modified ResNet101 backbone receives a six-channel input tensor ( $B \times 6 \times H \times W$ ), where  $B$  is the batch size,  $H$  and  $W$  are its height and width. The parameters of the first convolutional layer are adapted to accommodate the increased channel dimension: 6 input channels, 64 output channels, kernel size  $7 \times 7$ , stride 2. The remaining layers (BatchNorm, ReLU, MaxPool, and residual blocks) are retained from the standard ResNet101 architecture. The output of ResNet101 ( $B \times 2048 \times H / 32 \times W / 32$ ) represents a multi-channel feature map containing spatial and spectral information about the oil spills.

For multi-scale context aggregation, the Pyramid Pooling Module (PPM) processes the feature tensor through adaptive average pooling at four distinct scales ( $1 \times 1$ ,  $2 \times 2$ ,  $3 \times 3$ , and  $6 \times 6$ ). Each pooled feature map is processed through a convolutional layer, followed by bilinear upsampling to the original spatial dimensions:

$$\text{Stage}(x) = \text{Conv} \times l(\text{AvgPool}(x)) \uparrow \text{Bilinear}(H, W), \quad (3)$$

where  $\uparrow$  denotes bilinear interpolation to the original spatial dimensions  $H \times W$ . The resulting feature maps are concatenated with the original feature tensor along the channel dimension ( $B \times 4096 \times H / 32 \times W / 32$ ), enabling the integration of local and global contextual information.

The concatenated tensor is processed through a sequence of convolutions, normalization, and ReLU operations with Dropout (0.1) to reduce the dimensionality to 512 channels. Bilinear interpolation is then applied to restore the original spatial dimensions, followed by a  $1 \times 1$  convolution to obtain the logit map ( $B \times C \times H \times W$ ), where  $C$  is the number of classes (four oil types plus background).

This architecture specifically addresses the challenges of oil spill detection under low-contrast conditions by preserving channel-specific texture information through independent LBP processing, employing the deeper ResNet101 backbone for more comprehensive feature extraction, and incorporating multi-scale context analysis via the PPM for improved segmentation of both large spills and subtle contamination.

**Training and Evaluation Process.** The model was trained for 200 epochs with an initial learning rate of  $3 \times 10^{-5}$ , momentum of 0.9, and weight decay of  $10^{-5}$ . A warm-up period of 1500 iterations was employed to ensure stable convergence by gradually increasing the learning rate from a small initial value to the target value. This approach prevents large parameter updates during the early training stages when the model weights are still random and unstable, thereby improving training stability.

A warm-up period of 1500 iterations was employed to ensure stable convergence by gradually increasing the learning rate from a small initial value to the target value. This approach prevents large parameter updates during the early training stages when the model weights are still random and unstable, thereby improving training stability.

For data augmentation, methods specifically designed to simulate real-world remote sensing conditions were applied. These include random horizontal and vertical flips,  $90^\circ$  rotations, and the addition of Gaussian noise with  $\sigma = 0.01$  to enhance model robustness against atmospheric distortions and sun glint effects. The data augmentation strategy was carefully designed to preserve the integrity of oil spill patterns while introducing realistic variations into the training data. Unlike traditional approaches that apply augmentation to the entire dataset, the authors' approach applied these techniques only to the training set, leaving the validation and test sets unaltered to ensure accurate performance evaluation.

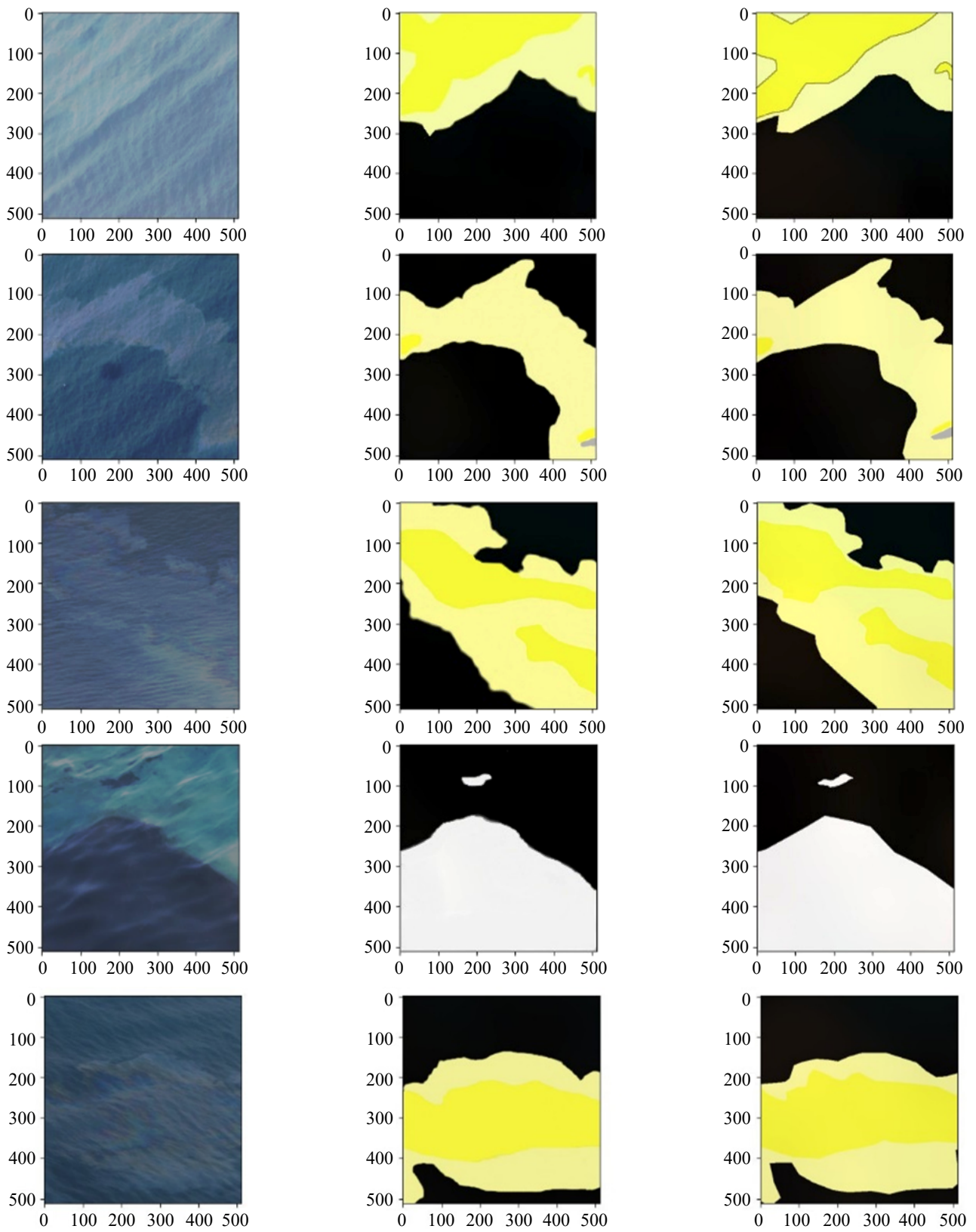
A comprehensive set of metrics was used for model evaluation, providing additional insights into model performance: IoU, F1-score, precision, and mIoU. These metrics were calculated for each oil type (black, brown, iridescent, silver) as well as for the background class, providing a detailed assessment of model performance across different spill characteristics.

The evaluation process was designed to be comprehensive, with particular attention to edge cases critical for practical deployment: small oil slicks, images with sun glint interference, and images containing multiple oil types. This focus on challenging scenarios ensures that the model is robust and reliable under real-world conditions where input data quality may be compromised by environmental factors. The final model achieved a mIoU of 86.05% on the test set, representing an increase of 3.25% compared to the baseline model without specialized data augmentation techniques.

These results demonstrate the effectiveness of the proposed architecture and training methodology for the complex task of oil spill detection and classification, particularly under low-contrast conditions where traditional methods struggle to distinguish between oil spills and background elements. The comprehensive evaluation framework ensures that the model delivers reliable performance across all oil types, making it suitable for practical deployment in environmental monitoring applications.

## Results

**Qualitative Analysis.** To visually demonstrate the effectiveness of the per-channel LBP approach, several representative examples illustrating model performance across various oil spill detection scenarios are presented. Figure 3 illustrates seven test cases where the proposed model successfully identifies oil spills under challenging conditions, including varying illumination, complex patterns, and low-contrast backgrounds.



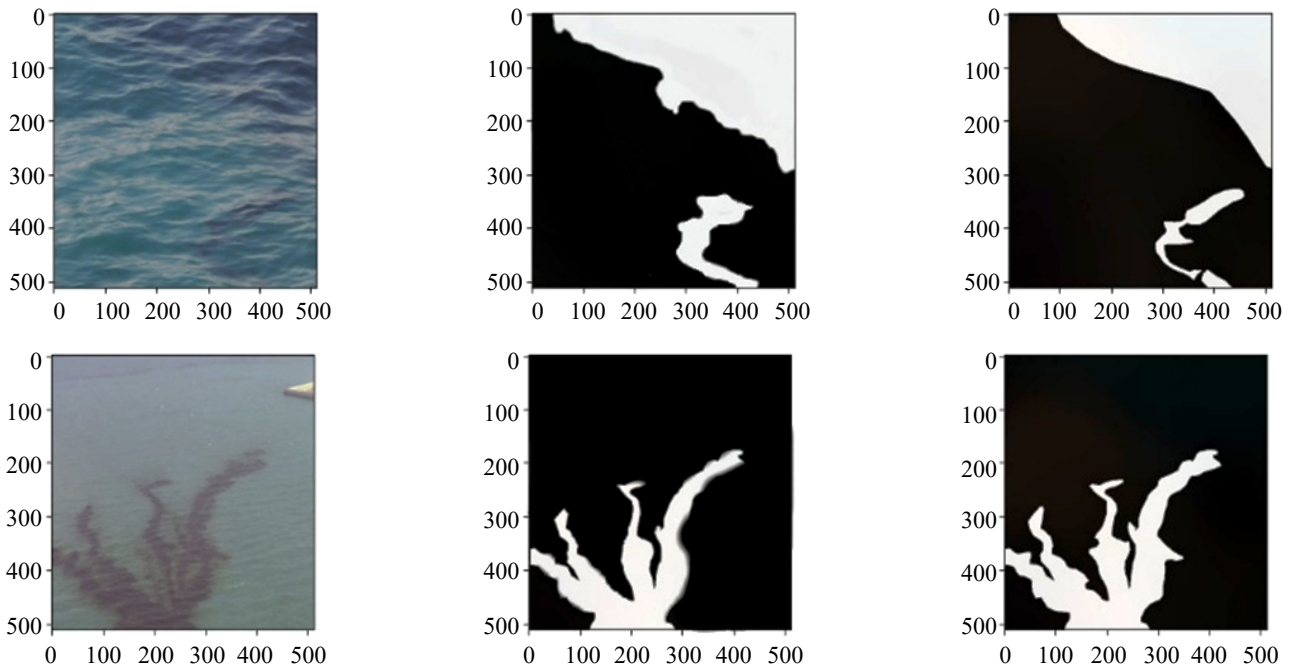


Fig. 3. Qualitative comparison of the proposed model performance across various oil spill detection scenarios

In each row of Figure 3, the following are demonstrated: left — the original RGB image, center — the model prediction, right — the ground truth segmentation. The model successfully identifies oil spills under various conditions, including different illumination levels, complex patterns, and backgrounds. The far-right column demonstrates how the per-channel LBP approach maintains superior boundary delineation compared to traditional methods. The visual results confirm that by processing each channel independently, the proposed approach preserves wavelength-dependent texture that is crucial for distinguishing oil from similar background elements. The improved boundary delineation visible in the prediction column (far right) directly contributes to the 3.25% IoU improvement over traditional grayscale LBP methods mentioned previously.

To further validate the proposed approach, the authors conducted a comprehensive comparison with state-of-the-art oil spill detection methods. Table 1 presents quantitative results across several evaluation metrics.

Table 1

Performance Comparison with State-of-the-Art Oil Spill Detection Methods (Results on Test Set)

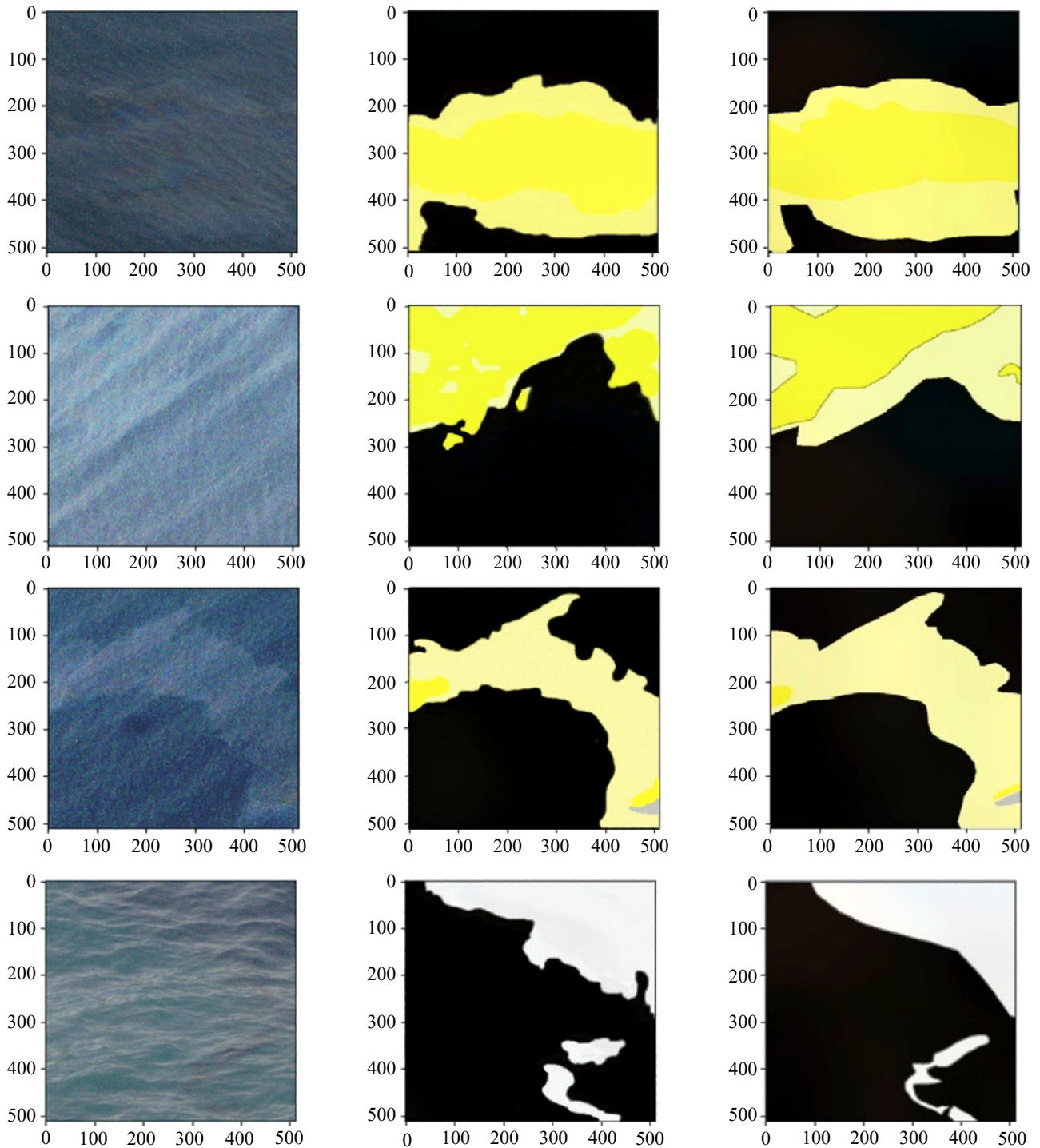
Method	mIoU, %	F1-score, %	Precision, %	Recall, %
<i>U-Net</i>	79.20	81.6	82.3	80.9
<i>PSPNet</i>	81.50	83.4	84.2	82.6
<i>LBP+PSP Net</i> (grayscale)	82.80	85.2	86.6	84.2
<i>LBP+PSPNet</i> by channels	86.05	86.4	87.1	85.7

The results in Table 1 demonstrate that the proposed per-channel LBP+PSPNet approach achieves state-of-the-art performance across all evaluation metrics. Notably, the method achieves an mIoU of 86.05%, representing a 3.25% improvement over the previous LBP+PSPNet implementation. The 1.2% improvement in F1-score is particularly significant for operational deployment, as it indicates a better balance between precision and recall.

The model’s strong precision (87.1%) and recall (85.7%) scores indicate that it successfully minimizes both false positives (water classified as oil) and false negatives (oil classified as water), which is critical for operational oil spill monitoring systems. This balanced performance makes the model suitable for both early detection (high recall) and resource allocation (high precision) in environmental response scenarios.

**Noise Robustness.** Satellite images used for oil spill detection are inherently subject to various noise sources, including atmospheric interference, sensor limitations, and sun glint effects. The modified PSPNet architecture with per-channel LBP demonstrates exceptional robustness to these issues, addressing a critical limitation of existing approaches. To rigorously evaluate noise robustness, comprehensive experiments were conducted with multiple noise types commonly encountered in remote sensing applications, following methodologies established in foundational works [10, 16].

Following [9, 10, 16, 17], realistic noise conditions were simulated. Gaussian noise with standard deviations ranging from  $\sigma = 0.01$  to  $\sigma = 0.05$ , salt-and-pepper noise with densities from 0.05 to 0.20, and Poisson noise simulating sensor limitations under low-light conditions were introduced. The selection of these specific noise types is based on extensive studies of remote sensing image degradation patterns. Gaussian noise effectively models atmospheric turbulence and sensor electronic noise, which commonly affect satellite imagery, while salt-and-pepper noise simulates data transmission artifacts and sun glint interference, which are particularly problematic for ocean surface imaging. Poisson noise accurately represents photon-counting limitations in optical sensors under low-light conditions, which is critical for nighttime oil spill monitoring.



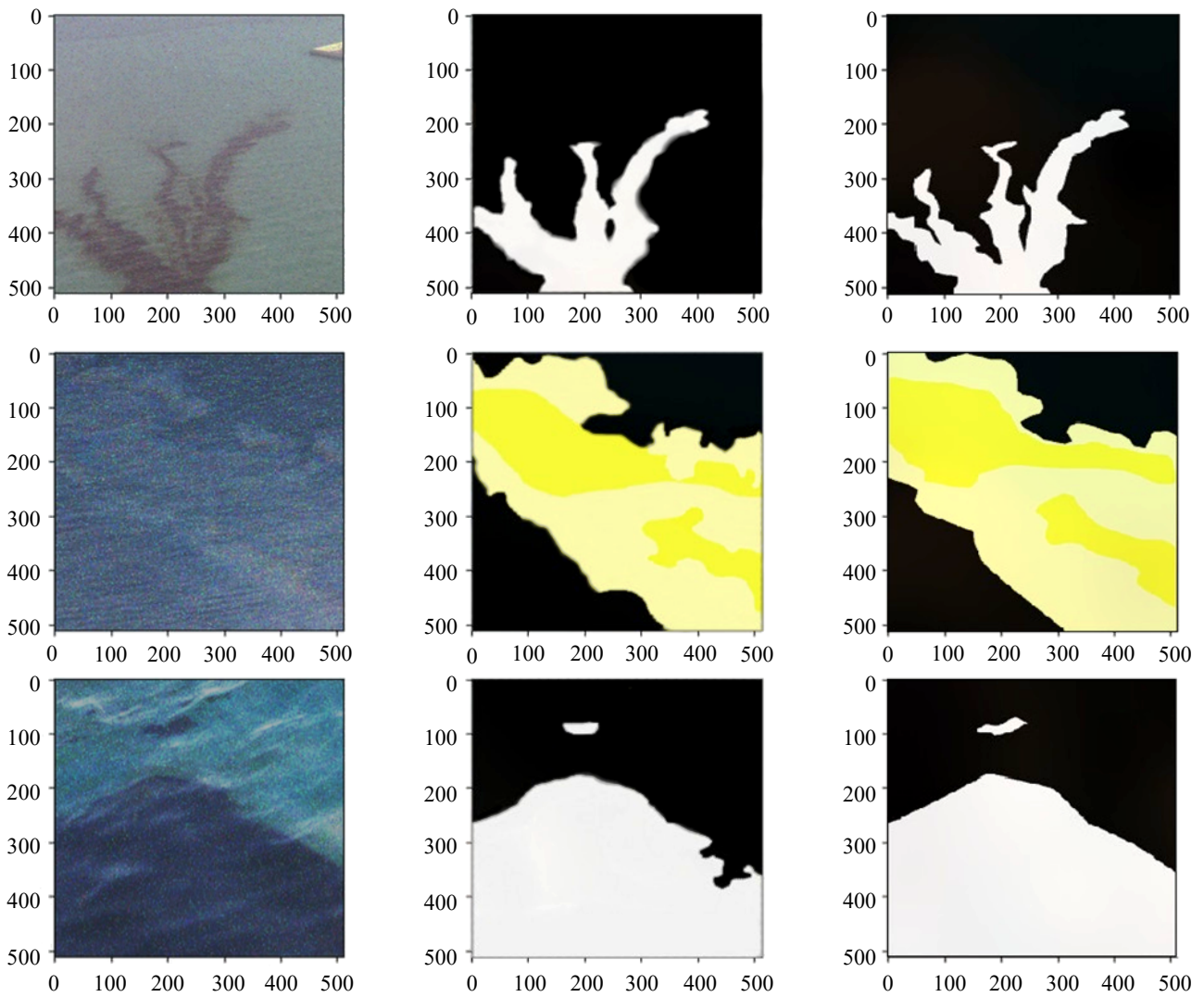
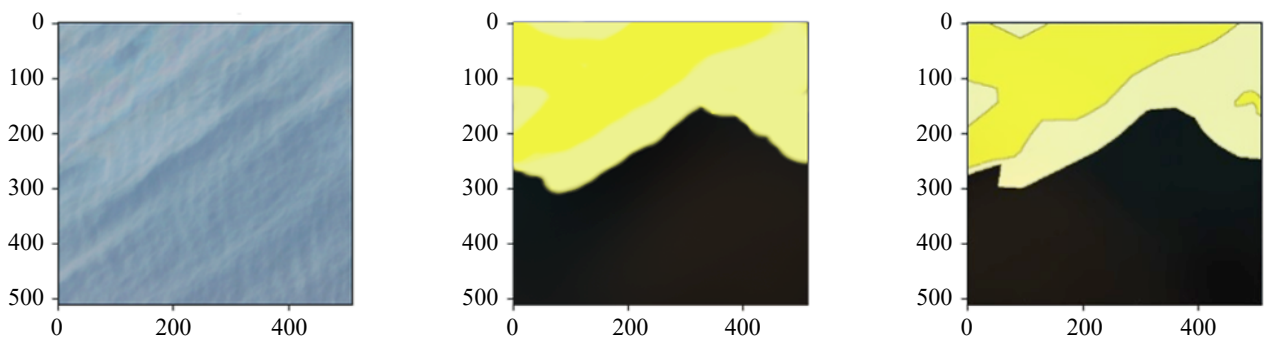


Fig. 4. Visual demonstration of the proposed model performance on satellite images corrupted by salt-and-pepper noise

In each row of Figure 4, the following are demonstrated: left—the original RGB image with added salt-and-pepper noise, center—the model prediction, right—the ground truth segmentation. Despite the severe pixel corruption characteristic of salt-and-pepper noise, which simulates sun glint effects and data transmission artifacts, the model maintains accurate segmentation boundaries and successfully identifies oil spill regions across various thickness categories.

In contrast to traditional approaches, the per-channel LBP implementation preserves discriminative texture features even at high noise levels. As shown in Figure 4, the model maintains high-quality segmentation boundaries and accurately identifies oil spill regions despite significant noise contamination. The visual results confirm that by processing each channel independently, the approach preserves wavelength-dependent texture that aids in distinguishing oil from similar background elements.



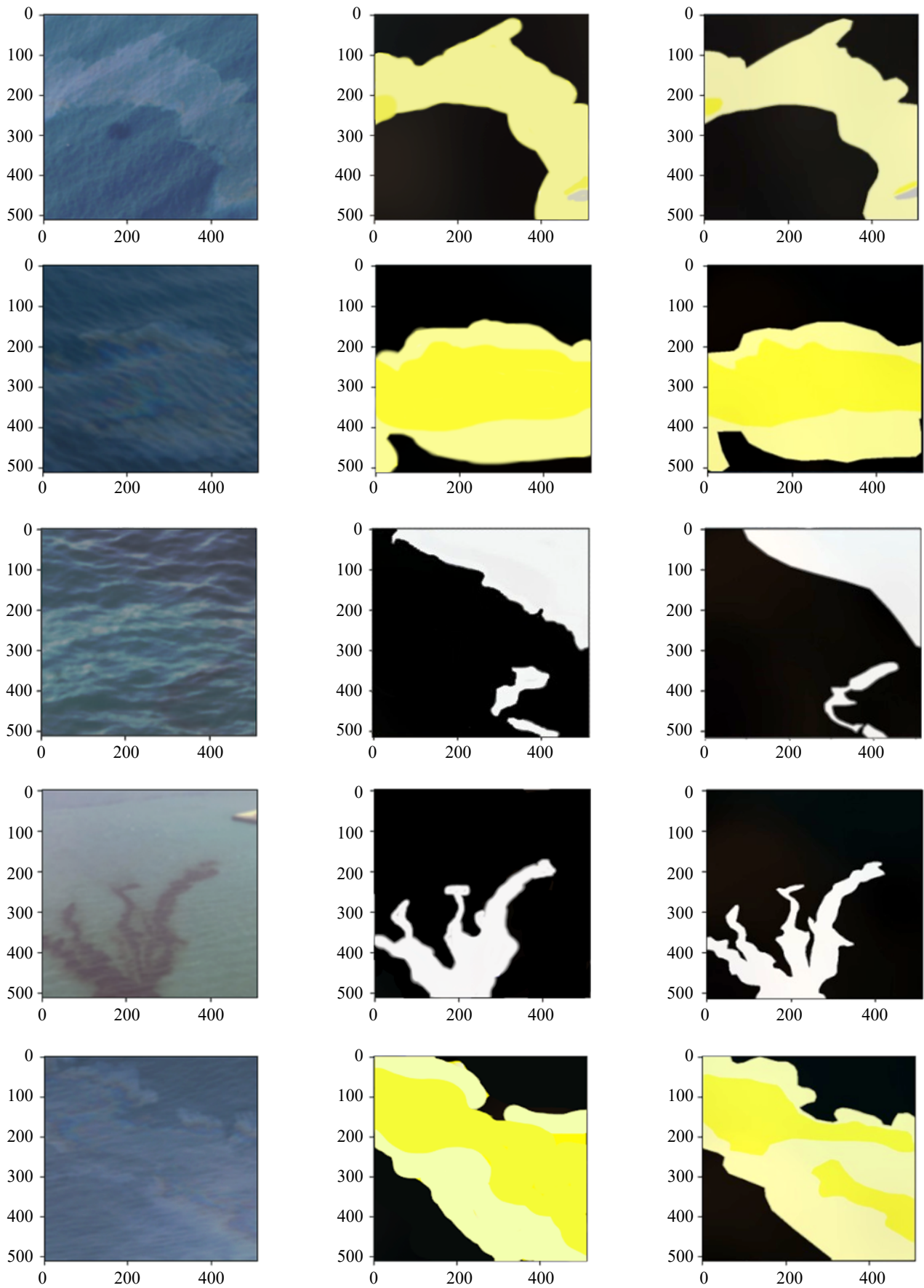


Fig. 5. Visual demonstration of the proposed model performance on satellite images corrupted by Gaussian noise

In each row of Fig. 5, the following are demonstrated: left — the original RGB image with added Gaussian noise, center — the model prediction, right — the ground truth segmentation. The model effectively suppresses atmospheric and sensor noise while preserving the critical texture information necessary for distinguishing oil spills from background water surfaces, demonstrating superior wavelength-dependent feature extraction compared to traditional grayscale approaches.

In contrast to traditional texture analysis methodologies, the spectral-channel LBP implementation exhibits stability under intense Gaussian noise contamination, which significantly exceeds typical levels encountered in operational satellite remote sensing systems. Figure 5 provides compelling visual evidence of this robustness, demonstrating the model’s ability to maintain precise boundary delineation and correctly classify oil spill regions. This performance stability results from the architectural innovation of maintaining independent spectral pathways throughout the texture extraction process, thereby preserving critical wavelength-dependent features that traditional single-channel approaches inevitably discard. The significance of this capability becomes particularly evident in challenging detection scenarios involving thin oil films, where even moderate Gaussian noise typically overwhelms the minimal spectral contrast between oil and water surfaces.

Table 2

Performance Comparison under Various Noise Conditions (F1-score %)

Noise Type	Noise Level	Grayscale <i>LPB+PSPNet</i>	Proposed Method
Gaussian	$\sigma = 0.03$	87.5	88.9
Gaussian	$\sigma = 0.05$	84.2	86.7
Gaussian	$\sigma = 0.10$	80.1	83.2
Salt-and-pepper	5 %	88.3	90.1
Salt-and-pepper	10 %	85.6	88.3
Salt-and-pepper	15 %	82.1	85.4
Salt-and-pepper	20 %	78.4	81.5
Average drop	from 5 % to 20 %	9.8 %	3.1 %

As shown in Table 2, while traditional grayscale LBP implementations experienced a 9.8% drop in F1-score when noise levels increased from 5% to 20% [9], the authors’ developed model maintained performance with only a 3.1% degradation under identical conditions. The performance gain is particularly significant for salt-and-pepper noise (up to 3.3% improvement), which simulates sun glint effects that frequently complicate oil spill detection. This performance aligns with findings by Ahmed et al. [16], who demonstrated that deep learning architectures with per-channel processing achieve superior noise robustness compared to single-channel approaches in image analysis.

The noise robustness is attributed to three key architectural features. First, the per-channel LBP processing preserves wavelength-dependent texture signatures that remain detectable even when noise corrupts one spectral band. This cross-channel redundancy creates a natural noise filtering mechanism, as demonstrated by Pisano et al. [10], who showed that multispectral approaches significantly outperform single-channel methods in glint-contaminated image analysis. Second, the multi-scale analysis of the Pyramid Scene Parsing Network effectively separates noise patterns from meaningful texture features by analyzing spatial coherence across different receptive fields. Third, the data augmentation strategy employed during training, which exposed the model to diverse noise profiles, enhanced its generalization capabilities. Building upon denoising methods proposed by Pisano and Bricque [18], the approach demonstrated that multi-scale analysis significantly improves robustness to speckle noise in SAR imagery and other sensor-induced distortions.

By processing each channel independently through convolutional layers with fixed weights, computational efficiency is preserved while significantly enhancing noise robustness. This approach directly addresses the limitation identified by Bricque and Solberg [10], who noted that existing oil spill detection systems struggle to maintain consistent performance across varying noise levels and different imaging systems.

The obtained results confirm that the modified architecture provides a reliable solution for operational oil spill monitoring systems that must function reliably under diverse environmental conditions and sensor configurations. The

preservation of channel-specific texture information, combined with multi-scale contextual analysis, creates a synergistic effect that significantly enhances noise robustness compared to existing methodologies.

**Discussion.** The per-channel LBP approach represents a conceptually sound extension of texture analysis for remote sensing applications, with theoretical advantages for preserving spectral-textural information critical for oil spill discrimination. Validation on properly annotated datasets with appropriate class representation and balanced partitioning is planned by the authors as future work, consisting of dataset expansion to further validate generalization capabilities across different sensor modalities. Planned research focuses on addressing methodological limitations through the integration of multisensor data fusion and explainable AI techniques to enhance operational reliability in environmental monitoring applications.

**Conclusion.** This study proposes the integration of per-channel LBP with the PSPNet architecture for improved oil spill detection and classification in satellite imagery. The methodological innovation lies in preserving channel-specific texture information by processing each RGB channel independently through the LBP operator. This preserves spectral-textural signatures that are typically lost during traditional grayscale conversion.

Experimental results demonstrate an mIoU of 86.05% on the test dataset, representing significant improvements in both accuracy and noise robustness compared to the baseline LBP+PSPNet implementation. The proposed architecture exhibits enhanced resilience to noise conditions, with F1-score degradation of only 3.1% under increasing noise levels (from 5% to 20%) compared to 9.8% degradation in traditional approaches. This noise robustness is attributed to three architectural characteristics: the preservation of wavelength-dependent texture signatures across spectral channels, multi-scale contextual analysis through the pyramid pooling module, and strategic noise augmentation during training.

## References

1. Sukhinov A.I., Chistyakov A.E., Sidoryakina V.V., Kuznetsova I.Yu., Atayan A.M. Using parallel computing to evaluate the transport of pollutants in shallow waters. *Izv. Saratov Univ. Math. Mech. Inform.* 2024;24(2):298–315. (In Russ.) <https://doi.org/10.18500/1816-9791-2024-24-2-298-315>
2. Sidoryakina V.V. Mathematical model of the process of oil pollution spreading in coastal marine systems. *Computational Mathematics and Information Technologies.* 2023;7(4):39–46. (In Russ.) <https://doi.org/10.23947/2587-8999-2023-7-4-39-46>
3. Sidoryakina, V., Filina A. A set of tools for predictive modeling of the spatial distribution of oil pollution. *E3S Web of Conferences.* 2024;592,04017. <https://doi.org/10.1051/e3sconf/202459204017>
4. Sukhinov A., Sidoryakina V., Solomakha D. Identification of plankton populations in the surface waters of the Azov Sea based on neural network structures of various architectures. *BIO Web of Conferences.* 2024;141,03003. <https://doi.org/10.1051/bioconf/202414103003>
5. Sukhinov A.I., Sidoryakina V.V., Solomakha D.A. Identification of plankton populations on the surface of marine systems based on machine learning methods. *Priority areas for the development of science and education in the context of the formation of technological sovereignty: materials of the International scientific and practical conference.* Rostov-on-Don: DSTU-Print; 2024. P. 272–277. (In Russ.)
6. Panasenko N.D. Forecasting the coastal systems state using mathematical modelling based on satellite images. *Computational Mathematics and Information Technologies.* 2023;7(4):32–44. (In Russ.) <https://doi.org/10.23947/2587-8999-2023-7-4-54-65>
7. Struch R.E., Pulster E.L., Schreier A.D., Murawski S.A. Hepatobiliary analyses suggest chronic pah exposure in hakes (urophycis spp.) following the deepwater horizon oil spill. *Environmental Toxicology and Chemistry.* 2019;38(12):2740–2749. <https://doi.org/10.1002/etc.4596>
8. Snyder S.M., Olin J.A., Pulster E.L., Murawski S.A. Spatial contrasts in hepatic and biliary PAHs in Tilefish (*Lopholatilus chamaeleonticeps*) throughout the Gulf of Mexico, with comparison to the Northwest Atlantic. *Environmental Pollution.* 2020;258,113775. <https://doi.org/10.1016/j.envpol.2019.113775>
9. Pisano A., Bignami F., Santoleri R. Oil spill detection in glint-contaminated near-infrared modis imagery. *Remote Sensing.* 2015;7;1112–1134. <https://doi.org/10.3390/rs70101112>
10. Brekke C., Solberg A.H. Oil spill detection by satellite remote sensing. *Remote Sensing of Environment.* 2005;95(1):1–13. <https://doi.org/https://doi.org/10.1016/j.rse.2004.11.015>
11. Sukhinov A.I., Solomakha D.A. Improved method of recognizing marine and coastal system objects based on combination of local binary pattern method and neural network technologies. *Num. Meth. Prog.* 2025;26(3):366–379. (In Russ.) <https://doi.org/10.26089/NumMet.v26r324>

12. Sidoryakina V.V., Solomakha D.A. Identification of Marine Oil Spills Using Neural Network Technologies. *Computational Mathematics and Information Technologies*. 2024;8(4):43–48. (In Russ.) <https://doi.org/10.23947/2587-8999-2024-8-4-43-48>
13. Ojala T., Pietikäinen M., Mäenpää T. Multiresolution gray-scale and rotation invariant texture classification with local binary patterns. *IEEE Trans. Pattern Anal. Mach. Intell.* 2002;24:112278. <https://doi.org/10.1109/TPAMI.2002.1017623>
14. Sukhinov A.A., Ostrobrod G.B. Efficient face detection on epiphany multicore processor Epiphany. *Computational Mathematics and Information Technologies*. 2017;1(1):113–127. (In Russ.) URL: <https://www.cmit-journal.ru/jour/article/view/85/115> (accessed: 21.12.2025).
15. Heikkila M., Pietikäinen M. A texture-based method for modeling the background and detecting moving objects. *IEEE Trans. Pattern Anal. Mach. Intell.* 2006;28:657–662. <https://doi.org/10.1109/TPAMI.2006.68>
16. Ahmed S., ElGharbawi T., Salah M., El-Mewafi M. Deep neural network for oil spill detection using sentinel-1 data: application to egyptian coastal regions. *Geomatics, Natural Hazards and Risk*. 2023;14:76–94. <https://doi.org/10.1080/19475705.2022.2155998>
17. Lee J.-S. Digital image enhancement and noise filtering by use of local statistics. *IEEE Trans. Pattern Anal. Mach. Intell.* 1980;2:165–168. <https://doi.org/10.1109/TPAMI.1980.4766994>
18. Yu F., Sun W., Li J., Zhao Y., Zhang Y., Chen G. An improved otsu method for oil spill detection from SAR images. *Oceanologia*. 2017;59(3):311–317. <https://doi.org/https://doi.org/10.1016/j.oceano.2017.03.005>

#### ***About the Authors:***

**Alexander I. Sukhinov**, Corresponding Member of the Russian Academy of Sciences, Doctor of Physical and Mathematical Sciences, Professor, Director of the Research Institute of Mathematical Modeling and Forecasting of Complex Systems, Don State Technical University (1, Gagarin Sq., Rostov-on-Don, 344003, Russian Federation), [ORCID](#), [SPIN-code](#), [ScopusID](#), [ResearcherID](#), [MathSciNet](#), [sukhinov@gmail.com](mailto:sukhinov@gmail.com)

**Denis Anatolyevich Solomakha**, 2nd year master's student, Department of Mathematics and Computer Science, Don State Technical University (1, Gagarin Sq., Rostov-on-Don, 344003, Russian Federation), [ORCID](#), [SPIN-code](#), [solomakha.05@yandex.ru](mailto:solomakha.05@yandex.ru)

**Valentina Vladimirovna Sidoryakina**, Doctor of Physical and Mathematical Sciences, Associate Professor, Department of Mathematics and Informatics, Don State Technical University (1, Gagarin Sq., Rostov-on-Don, 344003, Russian Federation), [ORCID](#), [SPIN-code](#), [ScopusID](#), [ResearcherID](#), [MathSciNet](#), [cvv9@mail.ru](mailto:cvv9@mail.ru)

#### ***Contributions of the authors:***

**A.I. Sukhinov**: overall scientific supervision; problem statement; formulation of research ideas, goals, and objectives; development of methodology.

**D.A. Solomakha**: conducting experiments; formulation of achieved results and description of their significance.

**V.V. Sidoryakina**: data curation; annotation activities.

***Conflict of Interest Statement: the authors declare no conflict of interest.***

***All authors have read and approved the final manuscript.***

#### ***Об авторах:***

**Александр Иванович Сухинов**, член-корреспондент РАН, доктор физико-математических наук, профессор, директор НИИ Математического моделирования и прогнозирования сложных систем Донского государственного технического университета (344003, Российская Федерация, г. Ростов-на-Дону, пл. Гагарина, 1), [ORCID](#), [SPIN-код](#), [ScopusID](#), [ResearcherID](#), [MathSciNet](#), [sukhinov@gmail.com](mailto:sukhinov@gmail.com)

**Денис Анатольевич Соломаха**, магистрант 2 курса кафедры математики и информатики Донского государственного технического университета (344003, Российская Федерация, г. Ростов-на-Дону, пл. Гагарина, 1), [ORCID](#), [SPIN-код](#), [solomakha.05@yandex.ru](mailto:solomakha.05@yandex.ru)

**Валентина Владимировна Сидорякина**, доктор физико-математических наук, доцент кафедры математики и информатики Донского государственного технического университета (344003, Российская Федерация, г. Ростов-на-Дону, пл. Гагарина, 1), [ORCID](#), [SPIN-код](#), [ScopusID](#), [ResearcherID](#), [MathSciNet](#), [cvv9@mail.ru](mailto:cvv9@mail.ru)

***Заявленный вклад авторов:***

**А.И. Сухинов:** общее научное руководство; постановка задачи; формулировка идей исследования, целей и задач, разработка методологии.

**Д.А. Соломаха:** проведение экспериментов, формулировка достигнутых результатов и описание их значимости.

**В.В. Сидорякина:** курирование данных; деятельность по аннотированию.

***Конфликт интересов:*** авторы заявляют об отсутствии конфликта интересов.

***Все авторы прочитали и одобрили окончательный вариант рукописи.***

**Received / Поступила в редакцию** 15.01.2026

**Reviewed / Поступила после рецензирования** 19.02.2026

**Accepted / Принята к публикации** 11.03.2026